Nuclear quadrupole interactions of ^{11}B in a LiB_3O_5 single crystal

2004 J. Phys.: Condens. Matter 16 445

(http://iopscience.iop.org/0953-8984/16/3/020)

INSTITUTE OF PHYSICS PUBLISHING JOURNAL OF PHYSICS: CONDENSED MATTER

J. Phys.: Condens. Matter **16** (2004) 445–453 PII: S0953-8984(04)65863-2

Nuclear quadrupole interactions of ^{11}B in a LiB_3O_5 single crystal

Sang Won Ahn[1,4], In Gyoo Kim[2], Sung Ho Choh[3] and Hee Jae Kang[1]

[1] Institute for Basic Science, Department of Physics, Chungbuk National University, Cheongju 361-763, Republic of Korea
[2] Basic Research Laboratory, Electronics and Telecommunications Research Institute, Taejon 305-350, Republic of Korea
[3] Department of Physics, Korea University, Seoul 136-701, Republic of Korea

Received 7 July 2003, in final form 10 December 2003
Published 9 January 2004
Online at stacks.iop.org/JPhysCM/16/445 (DOI: 10.1088/0953-8984/16/3/020)

Abstract

The rotation patterns of the nuclear magnetic resonance (NMR) spectra of an ^{11}B nucleus in a LiB_3O_5 (LBO) single crystal were measured in the three mutually perpendicular crystallographic planes at room temperature. We identified three centres denoted as B1, B2, and B3, each of which consists of four sets of ^{11}B NMR spectra originating from the chemically equivalent but magnetically inequivalent sites. The four sets belonging to each centre were properly classified in accordance with crystal symmetry and analysed. The principal values and principal axis orientations of the nuclear quadrupole coupling (NQC) tensors were determined for the first time. The centres B1, B2, and B3 were assigned to boron sites in the crystalline lattice of LBO by comparing the directions of the B–O bonds and the principal axes of the NQC tensor (**P**). The NQC constant (e^2qQ/h) and asymmetry parameter (η) were determined as follows: for B1, $e^2qQ/h = 2.615 \pm 0.005$ MHz and $\eta = 0.266 \pm 0.005$; for B2, $e^2qQ/h = 0.176 \pm 0.003$ MHz and $\eta = 0.584 \pm 0.003$; and for B3, $e^2qQ/h = 2.690 \pm 0.004$ MHz and $\eta = 0.204 \pm 0.003$.

1. Introduction

Lithium triborate (LiB_3O_5, LBO) crystals possess some excellent qualities, such as chemical stability, high damage threshold, small dielectric constant, and transparency far into the ultraviolet [1–3]. More than anything else, this boron oxide compound has a nonlinear optical (NLO) coefficient much larger than that of $KTiOPO_4$, which is another excellent NLO crystal discovered earlier. It has been shown that LBO is especially advantageous in the frequency conversion of high-power pulsed lasers [4, 5]. Practical applications for laser systems require radiation stability. Radaev *et al* [6] have shown that LBO meets the requirement in contrast

[4] Author to whom any correspondence should be addressed.

to such well-known materials as KH_2PO_4, $LiNbO_3$, $Ba_2NaNb_5O_{15}$, and $KTiOPO_4$. There are only a relatively small number of studies on the nuclear magnetic resonance (NMR) of LBO. Matsuo *et al* [7, 8] studied the ^{7}Li nuclear relaxation and line intensities as a function of temperature on both the crystal and glass phases of LBO. The nuclear quadrupole coupling (NQC) constant e^2qQ/h and the asymmetry parameter η of both ^{7}Li and ^{11}B in LBO were evaluated in our previous report [9].

In this work, we study the local structure around the boron atoms by investigating the quadrupole interactions of the ^{11}B nucleus in LBO. The quadrupole Hamiltonian parameters are more precisely determined than those in our previous report [9] by employing a sample with better quality and by achieving more accurate sample alignment. From the angular rotation patterns of ^{11}B NMR measured at room temperature, the principal values and principal axis orientations of NQC tensors are determined. The chemical bonding structure of B–O in LBO is discussed in terms of the present results and the electron-density-deformation (EDD) peak previously reported by others [3].

2. Crystal structure

The crystal structure of LBO was initially determined by König and Hoppe [10] and later verified by Shuqing *et al* [11]. It crystallizes in the form of orthorhombic space group $Pna2_1$ belonging to the point group $mm2$. A unit cell of this crystal contains four formula units and has lattice parameters $a = 0.8447$ nm, $b = 0.737\,89$ nm, and $c = 0.514\,08$ nm [3]. The symmetry elements of $Pna2_1$ are characterized by two glide planes and one screw axis, and there are four chemically equivalent but magnetically inequivalent sites for each crystallographically distinct atom.

Figure 1 shows the scheme of a set of B_3O_7 bonds, i.e. the three crystallographically distinct borons and the nearest oxygens surrounding the borons, and the ion positions are listed in table 1. The crystallographically distinct atoms are distinguished using the arabic numerals in parentheses. The main structural unit of LBO consists of two crystallographically distinct boron–oxygen triangles and one boron–oxygen tetrahedron. The B(1) atom lies almost within the planar triangles formed by the oxygens O(1), O(2)$^{\mathrm{i}}$, and O(3), and the B(3) atom by O(3), O(4)$^{\mathrm{iii}}$, and O(5)$^{\mathrm{v}}$. The two triangles possess a common vertex, the O(3) atom. On the other hand, the B(2) atom lies within the distorted tetrahedron surrounded by oxygens O(1), O(2), O(4)$^{\mathrm{iii}}$, and O(5)$^{\mathrm{iv}}$. The B(2) atom is linked to the B(1) and B(3) via O(1) and O(4)$^{\mathrm{iii}}$, respectively, and the Li atom is in the channel along the c axis. The boron sites as shown in figure 1 and listed in table 1 will be adopted as the representative site I among four chemically equivalent sites I to IV.

3. Experimental procedure

The LBO single crystals used in the present study were synthesized by the top seeded slow cooling method [1] at CASIX in China. In order to measure the angular dependence of the NMR spectra, a crystal sample was oriented by obtaining a number of x-ray-diffraction patterns. The sample was subsequently sawn with the faces perpendicular to the crystal axes a, b, and c, which are high symmetry directions. NMR spectra were taken from the as-grown LBO sample $3.0 \times 4.0 \times 5.0$ mm^3 along the a, b, and c axes, respectively.

The angular dependences of the NMR spectra were measured at room temperature by employing an MSL 200S pulsed NMR spectrometer, operating at a static magnetic field of 4.7 T. A single pulse, having width 1 μs, was used. The repetition time and the ring down delay time were about 10 min and 6 μs, respectively. The carrier frequency of the pulse was

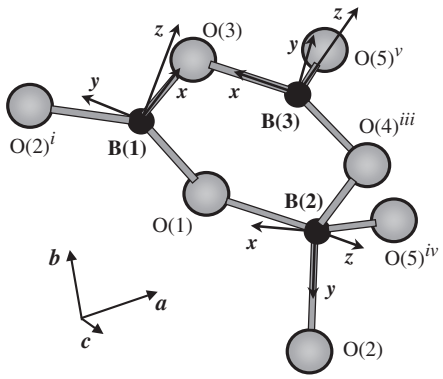

Figure 1. Practical scheme of three crystallographically distinct borons together with their nearest oxygens in the LiB_3O_5 lattice, showing the crystallogaphic axes **a**, **b**, and **c**. Each of **a**, **b**, and **c** corresponds to one eighth of its lattice constant, respectively. (See the footnote in table 1 for the meaning of the superscript symmetry codes.) The principal axes of the **P** tensor for centres B1, B2, and B3 (see text) have been represented as vectors with origins at B(1), B(2), and B(3), respectively.

Table 1. Ion positions of three crystallographically distinctive borons B(1), B(3), and B(2) and the nearest oxygens around the respective boron are given in units of a, b, and c lattice parameters in LiB_3O_5. (Taken from [3], except for five different choices of oxygens which were obtained from the original data by applying the superscript symmetry codes.)

Atoms[a]	x/a	y/b	z/c
	$B(1)O_3$ triangle		
B(1)	0.009 68	0.664 39	0.8098
O(1)	0.086 44	0.504 30	0.8022
$O(2)^{i}$	−0.116 33	0.704 90	0.6535
O(3)	0.058 09	0.798 16	0.9848
	$B(3)O_3$ triangle		
B(3)	0.157 05	0.748 59	0.1895
O(3)	0.058 09	0.798 16	−0.0152
$O(4)^{iii}$	0.238 98	0.590 24	0.1902
$O(5)^{v}$	0.161 02	0.874 96	0.3840
	$B(2)O_4$ tetrahedron		
B(2)	0.194 37	0.443 27	0.0063
O(1)	0.086 44	0.504 30	−0.1978
O(2)	0.116 33	0.295 10	0.1535
$O(4)^{iii}$	0.238 98	0.590 24	0.1902
$O(5)^{iv}$	0.338 98	0.374 96	−0.1160

[a] Symmetry codes: (i) $-x, 1-y, \frac{1}{2}+z$; (iii) $\frac{1}{2}-x, \frac{1}{2}+y, -\frac{1}{2}+z$; (iv) $-\frac{1}{2}+x, \frac{1}{2}-y, -1+z$; (v) $1-x, 1-y, -\frac{1}{2}+z$

varied in the range of $\omega_0/2\pi = 63.2$–65.2 MHz in order to excite all the satellite lines of ^{11}B NMR. The Larmor frequency of the ^{11}B nucleus was 64.2 MHz at the magnetic field **B** used for the experiment. The crystal alignments have been established within $\pm 0.2^\circ$ in the three

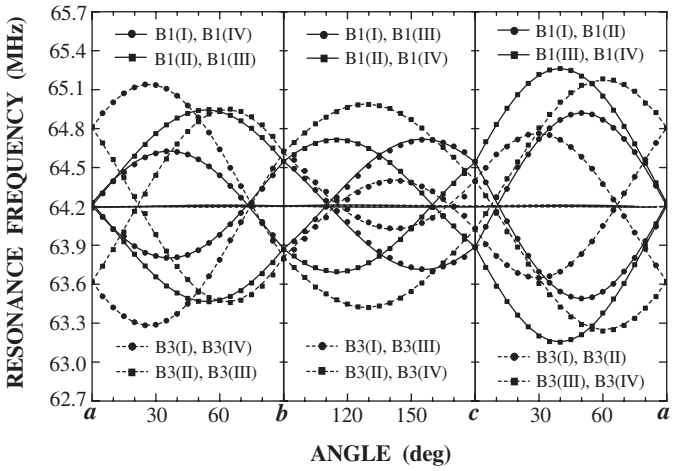

Figure 2. Angular dependence of the NMR spectra of the B1 and B3 centres observed at room temperature in the three crystallographic planes *ab*, *bc*, and *ca* of the LiB_3O_5 single crystal. The experimental NMR lines are represented by closed circles and squares while the solid curves for B1 and dotted curves for B3 are calculated ones using the EFG matrix in table 3.

planes by adjusting the crystal orientation in such a way as to achieve pairwise degeneracy of the NMR spectra arising from four chemically equivalent boron sites. The NMR spectra were recorded by varying the orientation of **B** in the three planes in steps of 5.0° with polar ϑ and the azimuthal angle ϕ ranging from 0° to 180°.

4. Results and discussion

The isotope ^{11}B is a quadrupolar nucleus with nuclear spin $I = 3/2$ and natural abundance of 80.42%. When the quadrupolar nucleus is located in the surroundings of the non-zero electric field gradient (EFG), it gives $2I$ resonance lines for the case where the nuclear quadrupole interaction perturbs the nuclear Zeeman energy levels. One of them is the central transition line ($|1/2\rangle \leftrightarrow |-1/2\rangle$) and the other two are satellite ones ($|3/2\rangle \leftrightarrow |1/2\rangle$ and $|-3/2\rangle \leftrightarrow |-1/2\rangle$). From the angular dependence of the NMR spectra, the three transitions between the nuclear spin states were clearly identified in the planes *ab*, *bc*, and *ca* as shown in figures 2 and 3. For an arbitrary direction of the magnetic field with respect to the crystal axes and planes, there are four sets of NMR lines arising from four chemically equivalent boron sites. If the magnetic field is restricted to the planes *ab*, *bc*, and *ca*, the four sets are pairwise degenerate and only two sets of NMR lines are observed. The non-degenerate pairs have mirror symmetry about the axes *a*, *b*, and *c* in each of the planes *ab*, *bc*, and *ca*. Finally, all four sets are completely merged into one when the magnetic field is along any of the *a*, *b*, and *c* axes.

The observable number of NMR spectra for a particular nucleus in LBO crystals is primarily determined by the symmetry of the point group *mm*2. However, the number is reduced when **B** is applied to a certain orientation in which the apparent magnetic symmetry is higher than that of the point group of the crystal lattice. Consequently, the pairs of sites, having twofold symmetry about the *c* axis and mirror symmetry across the *bc* and *ca* planes, become identical for **B** applied in the *ab*, *bc*, and *ca* planes, respectively. When **B** is applied parallel to each crystallographic axis, all four sites in *mm*2 become magnetically identical. However, all sites are magnetically distinct for **B** applied on skew planes which deviate from

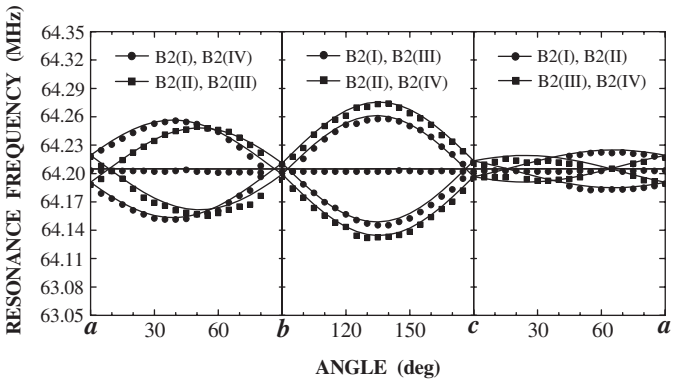

Figure 3. Angular dependence of the NMR spectrum of the B2 centre observed at room temperature in the three crystallographic planes *ab*, *bc*, and *ca* of the LiB_3O_5 single crystal. The experimental NMR lines are represented by closed circles and squares while the solid curves are calculated ones using the EFG matrix in table 3.

Table 2. Degenerate pairs, magnetic symmetry elements, and observable sets of NMR spectra arising from chemically equivalent sites I–IV.

Orientations of **B**	Degenerate pairs of NMR spectra	Magnetic symmetry elements	Observable sets of spectra
a, *b*, *c* axes	S_I, S_{II}, S_{III}, S_{IV}		1
ab plane	S_I, S_{IV}/S_{II}, S_{III}	$2 \parallel c$ (or $m \perp a$ and b)	2
bc plane	S_I, S_{III}/S_{II}, S_{IV}	$m \perp a$	2
ca plane	S_I, S_{II}/S_{III}, S_{IV}	$m \perp b$	2
Otherwise	None		4

the exact crystallographic planes. The degenerate aspects and the observable sets of NMR spectra S_I–S_{IV} arising from the respective sites I–IV are listed in table 2. The results are well in accord with those of NMR spectra as shown in figures 2 and 3.

In the case of a point defect located in a crystal lattice of the point group *mm*2, the degenerate aspects are also applicable to EPR spectra. Previously we obtained the same degenerate aspects of EPR spectra for four Cr^{3+} [12–14] and four Fe^{3+} [14–16] centres in $KTiOPO_4$ crystals with the same point group *mm*2 as that of LBO. The degenerate aspects are applicable to both NMR and EPR spectra and can be used as indicators for properly classifying the spectra originating from chemically equivalent but magnetically inequivalent sites and for examining the equivalency between several centres with similar NMR parameters due to very similar environments around the nuclei.

For the analysis of NMR spectra and their angular dependence, the Hamiltonian for an $I = 3/2$ nucleus system is:

$$H = H_Z + H_Q \tag{1}$$

where H_Z is the nuclear Zeeman term and H_Q the nuclear quadrupole interaction. The H_Q is expressed as follows:

$$H_Q = \mathbf{I} \cdot \mathbf{P} \cdot \mathbf{I} \tag{2}$$

by introducing the nuclear spin operator **I** and the NQC tensor **P** [17]. The **P** matrix is

symmetric and traceless and given by

$$\mathbf{P} = P \begin{pmatrix} \eta - 1 & 0 & 0 \\ 0 & -\eta - 1 & 0 \\ 0 & 0 & 2 \end{pmatrix} \tag{3}$$

in the principal axis system (x, y, z), where

$$P = \frac{e^2 q Q}{4I(2I-1)}. \tag{4}$$

The e^2qQ/h is the NQC constant and the η is the asymmetry parameter. Since the nuclear spin of ^{11}B is 3/2, $P = e^2qQ/12$. The parameter eq is just the EFG of largest magnitude (V_{zz}), and eQ describes the electrical shape of the nucleus and is a fixed number. By employing the EPR–NMR program which adapted the diagonalization algorithm of the **P** matrix representation of the Hamiltonian [18], we have determined the principal values and the principal axis orientations of the **P** tensor.

There are two possibilities for choosing a set of spectra in each of the planes ab, bc, and ca (see figures 2 and 3). Therefore, there are eight different ways to assign a set of spectra arising from four chemically equivalent ^{11}B sites in the three crystallographic planes. The agreement of the calculated NMR line positions with experimental ones is excellent for four particular choices of the spectra, while it fails completely for the others. The four sets corresponding to the good choices are defined as the centres B1(i) and B3(i) as shown in figure 2, and B2(i) in figure 3. The variables in parentheses i = I, II, III, IV indicate NMR spectra arising from four chemically equivalent boron sites as listed in table 2. The four sets yield the identical principal values of **P** tensors, whereas the orientations of the principal axes are different for each set. The rotation matrices, which transform the data of all symmetry-related sites into those of a reference site, could be found from the crystal symmetry of LBO. To obtain an accurate and meaningful determination of NMR parameters, a simultaneous fitting of all the experimental data set for chemically equivalent sites was carried out using the rotation matrices [18].

The final best fit of the principal values of the **P** tensors and the principal axes with respect to the crystallographic axes, a, b, c are listed in table 3 for the representative spectra B1(I), B3(I), and B2(I). The principal axis systems have been chosen to follow the convention $|P_{xx}| \leqslant |P_{yy}| \leqslant |P_{zz}|$, and have been represented in the right-handed coordinate system. The NQC constant and asymmetry parameter obtained from the principal values of the **P** tensor using equations (3) and (4) are also listed. The e^2qQ/h of the centre B1 is very similar to that of the centre B3 but approximately 14 times greater than that of the B2 centre.

To assign the centres B1, B2, and B3 to boron sites in the LBO crystal lattice, we have compared all four sets of the principal axes x, y, and z of the **P** tensor belonging to each centre with the B–O bond directions of LBO using the crystallographic data in table 1. One set of the spectra belonging to each centre, and providing a good match to the directions of the B–O bond, is selected as representative of B1(I), B3(I), and B2(I) as listed in tables 3 and 4. The principal x axis of both the centres B1 and B3 nearly coincides with the longest bond B(1)–O(3) in B(1)O_3 and B(3)–O(3) in B(1)O_3 planar triangles with 5.4° and 1.0° of the deviation angle ($\Delta\vartheta$), respectively. The asymmetry parameter η is expressed by $|P_{xx} - P_{yy}|/|P_{zz}|$ from equation (3) or $|V_{xx} - V_{yy}|/|V_{zz}|$ in the principal axis system of the EFG tensor, where $|P_{zz}| = (eQ/6)|V_{zz}|$ with the convention $|V_{xx}| \leqslant |V_{yy}| \leqslant |V_{zz}|$. Since the parameter eQ is a fixed number, each principal value (P_{ii}, $ii = xx, yy, zz$) is proportional to that (V_{ii}) of the EFG tensor. Therefore, the coincidence between the x axis with the smallest principal value of **P** and the longest B–O bond can be explained by the fact that the EFG is proportional to $1/r^3$. The largest O(1)–B(1)–O(2)$^{\mathrm{i}}$ and O(4)$^{\mathrm{iii}}$–B(3)–O(5)$^{\mathrm{v}}$ bond angles, formed by the short bonds in the triangles, are 123.32° and 124.92°, respectively. The smallest O(2)$^{\mathrm{i}}$–B(1)–O(3)

Table 3. Principal values and principal axis directions of the **P** tensor in polar coordinates (θ, ϕ) for the representative spectra of B1(I), B3(I), and B2(I), respectively. The quadrupole interaction parameters are also listed.

			Direction of principal axes	
Centres		Principal values	θ (deg)	ϕ (deg)
	$\lvert P_{xx}\rvert$	0.160 ± 0.001 MHz	52.6	73.4
B1(I)	$\lvert P_{yy}\rvert$	0.276 ± 0.001 MHz	112.8	114.6
	$\lvert P_{zz}\rvert$	0.436 ± 0.001 MHz	133.9	30.8
	e^2qQ/h	2.615 ± 0.005 MHz		
	η	0.266 ± 0.005		
	$\lvert P_{xx}\rvert$	0.178 ± 0.001 MHz	133.9	156.8
B3(I)	$\lvert P_{yy}\rvert$	0.270 ± 0.001 MHz	63.3	103.4
	$\lvert P_{zz}\rvert$	0.448 ± 0.001 MHz	117.5	28.6
	e^2qQ/h	2.690 ± 0.004 MHz		
	η	0.204 ± 0.003		
	$\lvert P_{xx}\rvert$	0.006 ± 0.001 MHz	127.8	172.8
B2(I)	$\lvert P_{yy}\rvert$	0.023 ± 0.001 MHz	59.8	236.0
	$\lvert P_{zz}\rvert$	0.029 ± 0.001 MHz	127.6	229.4
	e^2qQ/h	0.176 ± 0.003 MHz		
	η	0.584 ± 0.003		

and O(3)–B(3)–O(5)^{v} bond angles are 116.87° and 112.84°, respectively. The bond angles deviate slightly from the 120° formed by an isosceles triangle. If the triangles formed by the oxygens O(1), O(2)^{i}, and O(3) as well as O(3), O(4)^{iii}, and O(5)^{v} are isosceles, one of the principal axis directions will point to the normal of the triangular plane as observed in other crystals [19, 20] and calculations [21]. Such a normal direction of the $B(1)O_3$ and $B(3)O_3$ triangle provides a good match with the principal z axis of B1 and B3 with $\Delta\vartheta = 0.4°$ and 2.0°, respectively. In the two triangles, the longest and shortest bonds exist only in $B(1)O_3$ rather than $B(3)O_3$. Therefore, the $B(1)O_3$ triangle is more asymmetric than that of the $B(3)O_3$, and the B(1) yields a larger asymmetry parameter ($\eta = 0.266$) than that ($\eta = 0.204$) of B(3), as listed in table 3. The smaller P_{xx} (0.160 MHz) of B1 than that (0.178 MHz) of B3 is also in good agreement with EFG $\sim 1/r^3$. Since $e^2qQ/h = 12|P_{xx}|/(\eta - 1)h$ from equations (3) and (4), the larger value of e^2qQ/h for B3 can be understood from the fact that the larger $|P_{xx}|$ value of B3 overcomes the smaller values of η than those of B1. On the basis of the overall present NMR results, we have reached the conclusion that the centres B1 and B3 arise from the B(1) and B(3) boron site in LBO, respectively.

The bond angle of 112.94° formed by O(1)–B(2)–O(4)^{iii} is the largest for the distorted tetrahedron. The others range from 108.4° to 109.6° which are close to the typical angle 109.5° for a perfect tetrahedron. If the tetrahedron were perfect with cubic symmetry, the nuclear quadrupole interaction would be zero. The small distortion from the perfect tetrahedron yields the non-zero NQC constant of B(2), consequently its magnitude is much smaller than those of B(1) and B(3), as expected from the boron surroundings. The x axis with the smallest principal value is usually directed to the longest bond for the three-coordinated B1 and B3 centres, but not for the case in the B2 centre arising from the four-coordinated boron surroundings. One of the two long bonds, B(2)–O(2) (0.148 43 nm), provides a good match to the principal y axis with $\Delta\vartheta = 2.5°$ (see table 4).

Each B(1) and B(3) uses its sp^2 hybrid orbitals with three valence electrons to form bonds with oxygen atoms, and B(2) lends its four sp^3 hybrid orbitals with four oxygen atoms. It was

Table 4. Comparison of the B–O bond and plane-normal directions in $B(1)O_3$ and $B(3)O_3$ triangles, and the B–O bond in a $B(2)O_4$ tetrahedron with the principal axis directions of the **P** tensors for the representative spectra B1(I), B3(I), and B2(I), respectively (see figure 1).

Distances and directions in $B(1)O_3$					Principal axes of B1(I)		Angle[a]
Bond	d (nm)	θ (deg)	ϕ (deg)		θ (deg)	ϕ (deg)	$\Delta\vartheta$ (deg)
B(1)–O(3)	0.139 67	49.9	67.4	x	52.6	73.4	5.4
B(1)–O(2)[i]	0.136 66	125.9	164.4	y	112.8	144.6	21.6
Plane normal[b]		133.6	30.5	z	133.9	30.8	0.4
B(1)–O(1)	0.134 81	91.7	298.8				
Distances and directions in $B(3)O_3$					Principal axes of B3(I)		Angle[a]
Bond	d (nm)	θ (deg)	ϕ (deg)		θ (deg)	ϕ (deg)	$\Delta\vartheta$ (deg)
B(3)–O(3)	0.139 30	139.0	156.4	x	139.9	156.8	1.0
B(3)–O(5)[v]	0.136 75	43.0	87.9	y	63.3	103.4	23.7
Plane normal[c]		116.9	30.7	z	117.5	28.6	2.0
B(3)–O(4)[iii]	0.135 81	89.9	300.7				
Distances and directions in $B(2)O_4$					Principal axes of B2(I)		Angle[a]
Bond	d (nm)	θ (deg)	ϕ (deg)		θ (deg)	ϕ (deg)	$\Delta\vartheta$ (deg)
B(2)–O(1)	0.146 10	135.8	153.8	x	127.8	172.8	16.2
B(2)–O(2)	0.148 43	59.4	238.8	y	59.8	236.0	2.5
B(2)–O(5)[iv]	0.146 33	115.4	337.7	z	127.6	299.4	34.6
B(2)–O(4)[iii]	0.148 72	50.5	70.8				

[a] Angles between the B–O bond or the plane-normal directions and the principal axis directions of the **P** tensor.
[b] Normal direction to the face of the triangle formed by O(1), O(2)[i], and O(3).
[c] Normal direction to the face of the triangle formed by O(3), O(4)[iii], and O(5)[v].

proposed from the investigation of the EDD peak [3] that a pure σ-type bond is not realized along the shortest B(1)–O(1) or B(1)–O(2)[i] in the $B(1)O_3$ triangle, whereas the shape of the EDD peak of the longest B(1)–O(3) extends closely along the bond and the B(1)–O(3) bond is predominantly σ-type. It was additionally concluded [3] that the shape of the EDD peak of B(3)–O(3) extends almost along the bond and is more symmetrical than that of B(1)–O(3) about the bond, and the bond is purely σ-type. This agrees with our results in table 4 that the deviation angle of the B(3)–O(3) bond (1.0°) from the x axis is approximately five times smaller than that of B(1)–O(3) (5.4°). On the other hand, it was also shown by Radaev *et al* [3] that the EDD peaks of two long B(2)–O(2) and B(2)–O(4)[iii] bonds are more symmetrical about the bonds than those of the other two B(2)–O(1) and B(2)–O(5)[iv] bonds. This is also in good agreement with our result that the B(2)–O(2) bonds nearly coincide with the y axis. We have reached the conclusion from the overall facts that the centre B2 arises from the B(2) boron sites in LBO.

5. Conclusion

The degenerate aspects of the NMR spectra in table 2 can be used as the following indicators: (i) for properly classifying the spectra arising from chemically equivalent sites; (ii) for examining the equivalency between several centres. The nuclear quadrupole interaction parameters were determined as follows: for B1, $e^2qQ/h = 2.615 \pm 0.005$ MHz and $\eta = 0.266 \pm 0.005$; for B2, $e^2qQ/h = 0.176 \pm 0.003$ MHz and $\eta = 0.584 \pm 0.003$;

and for B3, $e^2qQ/h = 2.690 \pm 0.004$ MHz and $\eta = 0.204 \pm 0.003$. The centres B1, B2, and B3 were assigned to boron sites in LBO by comparing the directions of the B–O bonds and principal axes of **P** tensors. The present results support the chemical bonding structure suggested by Radaev *et al* that the longest B(1)–O(3) bond is predominantly a σ-type bond and B(3)–O(3) is an almost pure σ-type bond. The principal axes of the **P** tensors for B1, B2, and B3 can be used as complementary data with the EDD peak to elucidate the B–O bonding structures.

Acknowledgments

This work was supported in part by the Korea Science and Engineering Foundation through RCDAMP (1998–2000) and the Korea Research Foundation (Grant no KRF-2001-005-D20009).

References

[1] Chen C, Wu Y, Jiang A, Wu B, You G, Li R and Lin S 1989 *J. Opt. Soc. Am.* B **6** 616
[2] Lin S, Sun Z, Wu B and Chen C 1990 *J. Appl. Phys.* **67** 634
[3] Radaev S F, Maximov B A and Simonov V I 1992 *Acta Crystallogr.* B **48** 154
[4] Wu B, Chen N and Chen C 1989 *Opt. Lett.* **14** 1080
[5] Ebrahimzadel M, Robertson G and Dunn M H 1991 *Opt. Lett.* **16** 767
[6] Radaev S F, Muradyan L A, Malakhova L F, Rurak Y V and Simonov V I 1989 *Sov. Phys.—Crystallogr.* **34** 842
[7] Matsuo T, Shibasaki M, Katsumata T and Onoda Y 1994 *Japan. J. Appl. Phys.* **33** 3913
[8] Matsuo T, Shibasaki M, Saito N and Katsumata T 1996 *J. Appl. Phys.* **79** 1903
[9] Kim I G, Choh S H and Kim J N 1998 *J. Korean Phys. Soc.* **32** S669
[10] König H and Hoppe R 1989 *Z. Anorg. Chem.* **439** 842
[11] Shuqing Z, Chaoen H and Hongwu Z 1990 *J. Cryst. Growth* **99** 805
[12] Ahn S W, Choh S H and Kim J N 1995 *J. Phys.: Condens. Matter* **7** 667
[13] Ahn S W, Choh S H and Rudowicz C 1997 *Appl. Magn. Reson.* **12** 351
[14] Ahn S W and Choh S H 1999 *J. Phys.: Condens. Matter* **11** 3193
[15] Ahn S W, Choh S H and Choi B C 1995 *J. Phys.: Condens. Matter* **7** 9615
[16] Ahn S W and Choh S H 1998 *J. Phys.: Condens. Matter* **10** 341
[17] Weil J A, Bolton J R and Wertz J E 1994 *Electron Paramagnetic Resonance* (New York: Wiley) p 138
[18] Mombourquette M J, Weil J A and McGavin D G 1995 *Operation Instructions for Computer Program EPR–NMR Ver. 6.0* University of Saskatchewan, Canada
[19] Maurer H M, Schmidt P C and Weiss A 1997 *J. Mol. Struct.* **41** 111
[20] Kim I G and Choh S H 1999 *J. Phys.: Condens. Matter* **11** 8283
[21] Choh S H, Shin H W, Park I W, Ju H, Kim J H and Kim H J 2003 *J. Magn. Reson. Sco.* **7** 16